Geochemical Journal, Vol. 46, pp. e39 to e46, 2012

EXPRESS LETTER

East-west mantle geochemical hemispheres constrained from Independent Component Analysis of basalt isotopic compositions

HIKARU IWAMORI* and HITOMI NAKAMURA

Department of Earth and Planetary Sciences, Tokyo Institute of Technology,
2-12-1 Ookayama, Meguro-ku, Tokyo 152-8551, Japan

(*Received June 16, 2012; Accepted July 26, 2012; Online published August 21, 2012*)

In order to decipher the mantle geochemical heterogeneity that reflects material differentiation and circulation within the Earth, we examined mid-ocean ridge basalts (MORB), ocean island basalts (OIB) and arc basalts (AB), in terms of the radiogenic isotopic variability and its geographical distribution. It has been found that the Sr, Nd and Pb isotopic ratios of MORB, OIB and AB exhibit a two-dimensional structure, and are mostly distributed on the same compositional plane that is spanned by two independent components (IC1 and IC2). One of the two components (IC2) divides geochemically the mantle broadly into the Eastern and Western Hemispheres. Inspection of the geochemical nature of IC2 suggests that it may represent a fluid mobile component recycled through subduction zones. The mantle geochemical domain beneath the Eastern Hemisphere is enriched in the fluid mobile component, possibly by focused subduction towards the supercontinent Pangea which was surrounded by subduction zones. Although the present-day continents have been dispersed since then, the geochemical domain has seemingly been anchored to the asthenosphere without moving with the continents.

Keywords: mantle, isotope, domain, basalt, supercontinent

INTRODUCTION

Isotopic composition of the Earth's mantle reflect differentiation history of the planet, and based on its variability and spatial distribution, the global material cycling and the structure of mantle convection have been discussed (e.g., Hofmann, 1997). By examining compositions of mid-ocean ridge basalts (MORB) and ocean island basalts (OIB) as a "blood test" of the mantle, isotopic composition of the mantle has been surveyed over the globe to have discovered a large-scale geochemical domain termed "Dupal anomaly" in the Southern Hemisphere (Dupré and Allègre, 1983; Hart, 1984). Although the number of isotopic data used to map such domains has increased by two orders of magnitude since then, for example from 72 (Zindler *et al*., 1982) to 4288 (Iwamori *et al*., 2010) in the last 30 years, the spatial coverage of data with the oceanic basalts is still insufficient for resolving even a long-wavelength feature (e.g., a hemispherical structure).

In this study, the arc basalts (AB) in subduction zones, together with MORB and OIB, are incorporated into the mapping analyses in both geographical and compositional domains. AB fill the spatial gaps for the mapping analysis, especially along the Western to Southern Pacific and within the Eurasian and the American plates. Isotopic heterogeneity of pristine sub-arc mantle prior to addition of slab-derived materials has been discussed, e.g., in conjunction with the boundary between the Pacific Ocean-type and Indian Ocean-type mantle domains in the Western Pacific (Hickey-Vargas, 1998; Flower *et al*., 2001; Ishizuka *et al*., 2003; Nebel *et al*., 2007; Nakamura and Iwamori, 2009; Machida *et al*., 2009), whereas this study makes the first attempt to systematically resolve the whole globe using common geochemical criteria to MORB, OIB and AB. Combining the arc data with those from oceanic basalts, and using a multivariate analysis to clarify influences of the slab-derived materials on AB, we extract the composition of pristine sub-arc mantle. As a result, global geochemical domains appear primarily as east-west hemispheres, rather than north-south hemispheres (Hart, 1984) as has long been argued for. Based on the geochemical nature of the domains, as well as their spatial distribution that seems to have been anchored to the asthenosphere at least in the last several hundred million years, we discuss their origin and implications for mantle dynamics.

*Corresponding author (e-mail: hikaru@geo.titech.ac.jp)

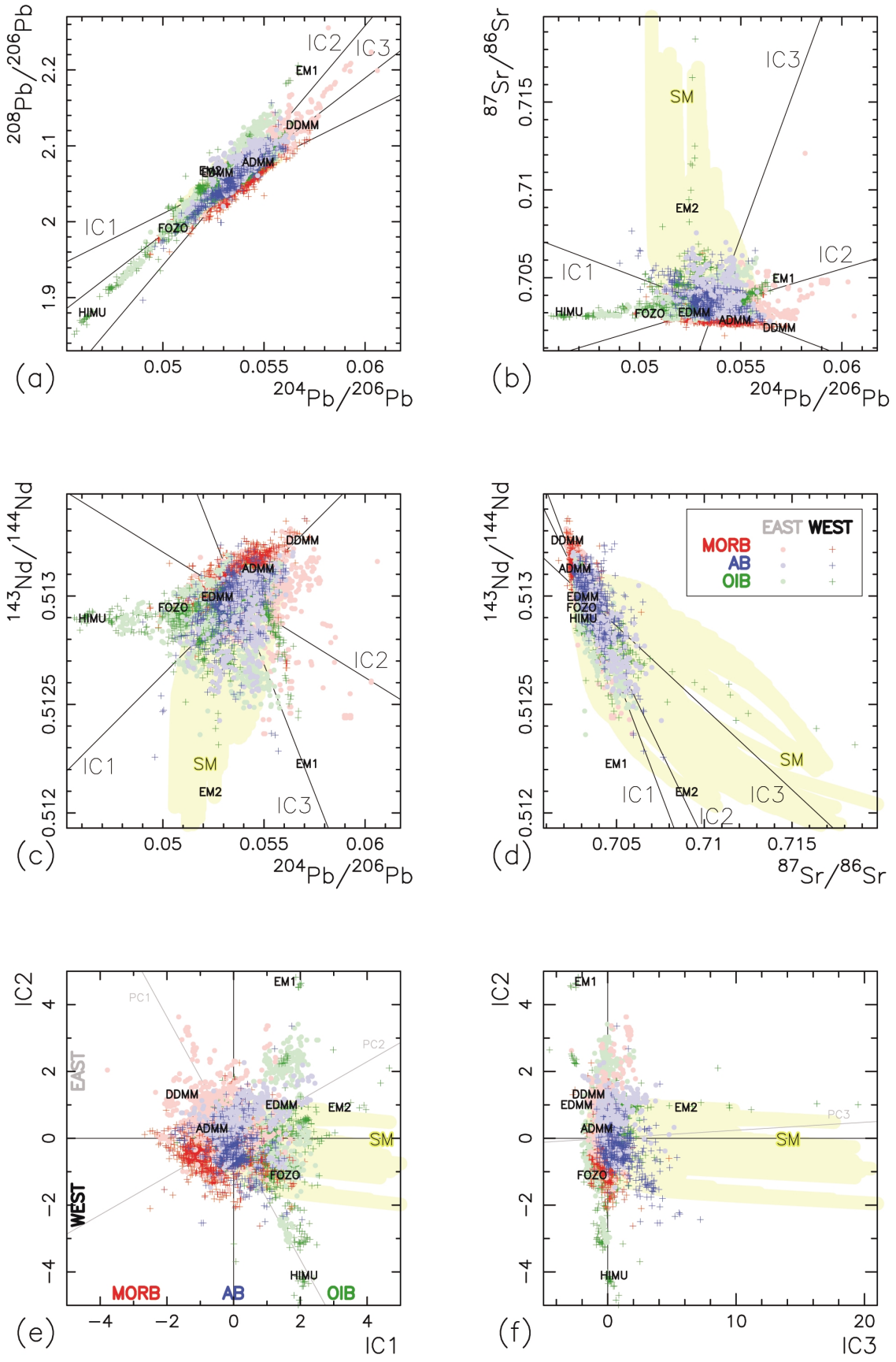
(a)
$^{208}Pb/^{206}Pb$
$^{204}Pb/^{206}Pb$
IC1
IC2
IC3
EM1
DDMM
ADMM
EDMM
FOZO
HIMU
(b)
$^{87}Sr/^{86}Sr$
$^{204}Pb/^{206}Pb$
SM
EM2
EM1
(c)
$^{143}Nd/^{144}Nd$
$^{204}Pb/^{206}Pb$
(d)
$^{143}Nd/^{144}Nd$
$^{87}Sr/^{86}Sr$
EAST WEST
MORB
AB
OIB
(e)
IC2
IC1
PC1
PC2
EAST
WEST
(f)
IC2
IC3
PC3

Fig. 1.

DATA AND METHOD

Unlike MORB and OIB, AB may not directly reflect inherent global features of the mantle, since the source mantle of AB is fluxed by local slab-derived materials associated with subduction (e.g., Plank and Langmuir, 1998; Pearce *et al*., 2005). In order to extract inherent variability of the mantle from AB, the compositional modification by slab-derived materials needs to be evaluated. For this sake, we first compare the isotopic composition of AB with those of MORB and OIB (Fig. 1), including total 5337 data (2773 MORB, 1515 OIB, 1049 AB from GEOROC [http://georoc.mpch-mainz.gwdg.de/georoc/] and PetDB [http://www.petdb.org, Lehnert *et al*., 2000] databases and Iwamori *et al*., 2010) with five isotopic ratios ($^{87}Sr/^{86}Sr$, $^{143}Nd/^{144}Nd$, $^{206}Pb/^{204}Pb$, $^{207}Pb/^{204}Pb$ and $^{208}Pb/^{204}Pb$) determined on the same sample. Since a high correlation coefficient between $^{206}Pb/^{204}Pb$ and $^{207}Pb/^{204}Pb$ (corrected for mass fractionation) is observed in some instrumental analyses to potentially interfere with geochemical correlations, while there is no significant correlation between $^{204}Pb/^{206}Pb$ and $^{207}Pb/^{206}Pb$ (Albarède *et al*., 2004), we work with the ^{206}Pb-normalized ratios in the following diagrams and statistical analyses as in Iwamori *et al*. (2010).

Figure 1 shows the isotopic variations of MORB, OIB and AB. Depending on which isotopic ratios are chosen, the discrimination among MORB, OIB and AB varies and is best seen in $^{204}Pb/^{206}Pb$ vs. $^{208}Pb/^{206}Pb$ (Fig. 1a) and $^{204}Pb/^{206}Pb$ vs. $^{143}Nd/^{144}Nd$ (Fig. 1c), whereas it is less obvious in $^{204}Pb/^{206}Pb$ vs. $^{87}Sr/^{86}Sr$ (Fig. 1b) and is rather obscured in $^{87}Sr/^{86}Sr$ vs. $^{143}Nd/^{144}Nd$ (Fig. 1d). This is because the data set has a planar structure within the five-dimensional isotope space as is demonstrated by Principal Component Analysis (PCA): the major plane, which is spanned by two principal components (PCs), accounts for 95.3% of the sample variance. The important and robust feature of the data structure is, therefore, that most of the MORB, OIB and AB data lie on the same plane. The third PC accounts for 4.0%. For example, the Pb–Nd isotopic plot (Fig. 1c) is roughly parallel to the major plane, and resolve well the major structure, whereas the Sr–Nd isotopic plot (Fig. 1d) is roughly perpendicular to the major plane, and clarifies the relationship between the major plane (exhibiting a linear "mantle array" in Fig. 1d) and the third component that extends towards a high Sr isotopic ratio.

Within this structure, MORB, OIB and AB are roughly discriminated as in Fig. 1, and AB broadly plot between MORB and OIB, which is seen in the Pb–Nd isotopic plot (Fig. 1c), reflecting the distinct mean values (e.g., $^{206}Pb/^{204}Pb = 18.425$ (MORB), 18.644 (AB), 19.001 (OIB), and $^{143}Nd/^{144}Nd = 0.513059$ (MORB), 0.512941 (AB), 0.512885 (OIB), respectively). In addition, when compared with MORB and OIB, AB plot slightly off the major plane (e.g., Fig. 1d): AB expand towards the compositional range of slab-derived materials with a high Sr isotopic ratio (yellow band labeled "SM" representing compositions of the slab-derived materials, see Appendix for more details), corresponding to a high mean $^{87}Sr/^{86}Sr$ ratio for AB (0.70385) relative to MORB (0.70292) and OIB (0.70372).

In order to clarify the relationship among MORB, OIB, AB and SM, i.e., the data structures in the multi-dimensional space with the five isotopic ratios, multivariate analyses are useful. Of these PCA has been regarded as the most efficient way to identify the mantle isotopic end-members (e.g., Zindler *et al*., 1982; Allègre *et al*., 1987; Blichert-Toft *et al*., 2005). However, the principal components (PCs) are independent only when the data constitute a joint Gaussian distribution, and this is clearly invalidated for the isotope compositions of oceanic basalts (Iwamori and Albarède, 2008). In this case, PCs do not form a set of independent vectors describing uniquely the isotopic variability.

Instead, we use Independent Component Analysis (ICA), a relatively new type of multivariate analysis that has been developed in the fields related to Information Science (Hyvärinen *et al*., 2001). ICA can be explained using an example of "blind source separation". Let us consider sounds from several instruments with independent waveforms, recorded simultaneously on multiple microphones distributed at arbitrary positions. Each microphone records a mixed sound from the instruments with a specific mixing proportion. From these records x, waveforms of the sound sources s and the mixing proportions A can be deduced based solely on non-Gaussianity inherited in the records x, without any a priori information on

Fig. 1. Isotopic compositions of oceanic and arc basalts. Mid-ocean ridge basalts (MORB, light or dark red), ocean island basalts (OIB, light or dark green), and arc basalts (AB, light or dark blue) are plotted with the isotopic ratios ((a) to (d)) or the independent components ((e) and (f)). In (e) and (f), the principal components (PCs) are also shown. Since PC1 and PC2 span the major plane to which PC3 is perpendicular, only PC1 and PC2 are shown in (e) while only PC3 is shown in (f). The data from the Eastern and Western Hemispheres are shown with different symbols, "solid circle" in light colors and "plus" in dark colors, respectively. "SM" represents the estimated compositional range of slab-derived materials (see Appendix), which overlaps with the data (thereby invisible) in Fig. 1a for Pb isotopes. Approximate location of conventional mantle geochemical end-members is also shown for HIMU, FOZO or C, A-DMM, D-DMM, E-DMM, EM1 and EM2, after Iwamori and Albarède (2008).

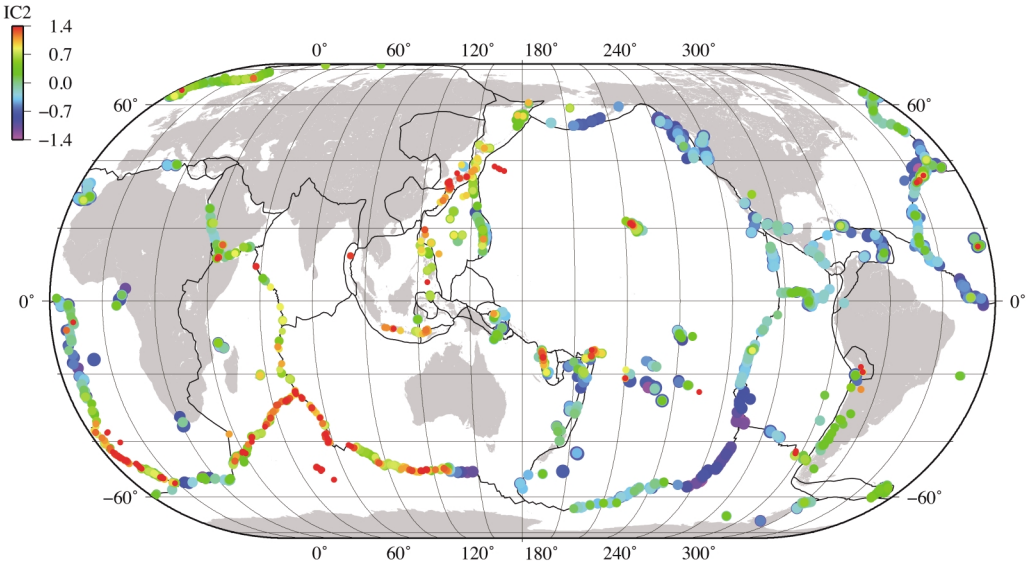

Fig. 2. Geographical distribution of IC2 value for oceanic and arc basalts. In each location, the variability is shown by the size of the color-coded symbols (smaller for the higher IC2 values).

s and *A*. This is what ICA exactly does to deduce the independent components (ICs), in this case waveforms of the sound sources hidden in the data. Although ICA is applicable to not only linear mixing but also non-linear problems, the correlations among the isotopic ratios in this study are sufficiently linear (as represented by the major plane in Fig. 1e), and linear ICA provides a good representation for the actual data.

In geochemical applications of ICA, source materials and processes with independent geochemical signatures (e.g., isotopic ratios) can be identified as ICs. In the case with the compositional space with isotopic ratios, the ICs are expressed as linear lines with specific slopes (Fig. 1). These slopes correspond to those of the independent base vectors that span the compositional space, so that the data can be explained uniquely by a combination of the base vectors. The obtained base vectors, i.e., ICs, are interpreted to deduce the actual processes, which could be for example mixing of independent geochemical end-members (such as those in Fig. 1: e.g., DMM, EM1, EM2, HIMU, FOZO) or variable degrees of isotopic fractionation (associated with variable degrees of parent-daughter differentiation and/or variable ages). Although the interpretation is non-unique, we will show that the geographical distribution of the IC value provides a rather unique constraint on the origin of the isotopic variability.

Results and Discussion

Applying ICA to the whole data set with MORB, OIB and AB, the three independent components (ICs) have been determined as in Fig. 1, which account for 99.3% of the sample variance. The projection with the ICs coordinate axes clarifies how IC1 and IC2 span the major plane that accounts for most of the sample variance (Fig. 1e) and that IC3 accounts for the data off the plane (Fig. 1f). Three important features appear in the IC domain. (1) In terms of IC1 (Fig. 1e), 95% of OIB, except for Hawaii and Iceland, plot on the positive side and 83% of MORB plot on the negative side except for those from the plume-influenced ridges such as Iceland, Azores, Galapagos and Red Sea (Iwamori *et al*., 2010), and AB plot close to zero with the mean IC1 = 0.109, roughly between OIB (mean IC1 = 0.873) and MORB (mean IC1 = –0.518). (2) IC2 generally separates the basalts into the eastern and western hemispheres irrespective of IC1 values or the type of basalts, MORB, OIB or AB (Figs. 1e and 2): approximately 77.9% of the basalts from the western hemisphere (200°W (=160°E) to 20°W in longitude) plot in the negative IC2 field, whereas approximately 73.2% from the remaining eastern hemisphere plot in the positive field (Fig. 1e). (3) AB plot slightly off the IC1-IC2 major plane and shifted towards a high IC3 (Fig. 1f). These features associated with IC1 to IC3 are examined in detail below.

It is noted that the obtained ICs and PCs are essentially the same as those obtained from only MORB+OIB (see Figs. 2e and 2f of Iwamori *et al*., 2010), because AB are close to the mean values of the whole or OIB+MORB dataset. It is also noted that the two major principal components (PC1 and PC2) plotted in Fig. 1e are oblique to IC1 and IC2, indicating that the data constitute a non-Gaussian joint distribution in which case the PCs are not independent (Iwamori and Albarède, 2008), and that the PCs discriminate neither the basalt types nor the geo-

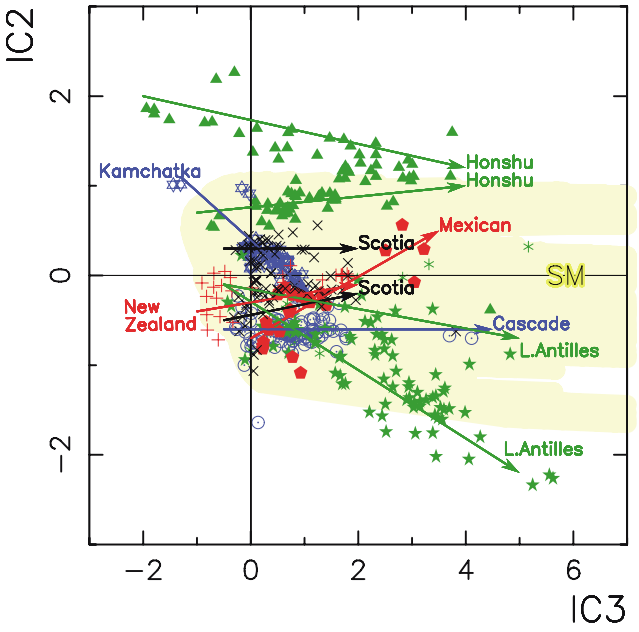

Fig. 3. IC3-IC2 trends for representative arcs. Arrows indicate the approximate linearized trends for Honshu (green triangle), Kamchatka (purple open star), Scotia (black cross), New Zealand (red plus), Cascade (purple open circle with a central dot), Mexican (red pentagon) and Lesser Antilles (green star). "SM" is the same as in Fig. 1.

graphical distribution.

IC1 has negative slopes in $^{87}Sr/^{86}Sr$–$^{204}Pb/^{206}Pb$ and $^{87}Sr/^{86}Sr$–$^{143}Nd/^{144}Nd$ spaces, whereas it exhibits a positive slope in $^{143}Nd/^{144}Nd$–$^{204}Pb/^{206}Pb$. The slopes of IC1 suggest that it originates from elemental fractionation associated with mantle melting which causes simultaneous increases in U/Pb, Th/Pb, Rb/Sr and Nd/Sm in melts and decreases of the ratios in residual peridotites (e.g., Beattie, 1993; Green, 1994; Salters and Longhi, 1999). Furthermore, these slopes can be compared quantitatively with differentiation-recycling models associated with melting (e.g., MORB-residual harzburgite recycling model (Christensen and Hofmann, 1994; Rudge *et al.*, 2005) or OIB-recycling model (McKenzie *et al.*, 2004)). Since the "melt component"-rich lithology (e.g., eclogite) is likely to be denser than the surrounding peridotitic portion in the mantle, it may accumulate near the base of the mantle convection system. The deep seated "melt component"-rich lithology contains more radiogenic elements (as U, Th and K are incompatible elements that are partitioned preferentially into melts) and produce heat to cause upwelling plumes to be the OIB source (e.g., Christensen and Hofmann, 1994; Nakagawa *et al.*, 2009), exhibiting positive IC1 signatures in OIB (Fig. 1e). On the other hand, a relatively shallow part of the mantle is depleted in such "melt component", resulting in negative IC1 signatures for MORB (Fig. 1e). These differentiation-recycling models may explain the IC1 feature (1) listed above.

IC2 has negative slopes in $^{143}Nd/^{144}Nd$–$^{204}Pb/^{206}Pb$ and $^{87}Sr/^{86}Sr$–$^{143}Nd/^{144}Nd$ spaces, whereas it exhibits a positive slope in $^{87}Sr/^{86}Sr$–$^{204}Pb/^{206}Pb$. The slope of IC2 has an opposite sign to that of IC1 in $^{143}Nd/^{144}Nd$–$^{204}Pb/^{206}Pb$ and $^{87}Sr/^{86}Sr$–$^{204}Pb/^{206}Pb$. These features indicate that IC2 originates from elemental fractionation with simultaneous increases (or decreases) in Pb/U, Pb/Th, Rb/Sr and Nd/Sm. Such fractionation can occur associated with aqueous fluid-mineral reactions (Brenan *et al.*, 1995; Keppler, 1996; Kogiso *et al.*, 1997) or hydrous melt-mineral reactions (Kessel *et al.*, 2005). Considering that IC2 constitutes one of the major base vectors, it must correspond to a significant prevailing process on Earth, which therefore suggests that aqueous fluid processes in subduction zones create the IC2 variation (Iwamori and Albarède, 2008). How these characteristics are related to the east-west geochemical hemispheres as in (2) raised above will be discussed later.

IC3 is characterized by a steep slope in the Pb–Sr plot (Fig. 1b) and a gentle slope in the Sr–Nd plot (Fig. 1d), both pointing roughly towards EM2 or along SM with an extremely high Sr isotopic ratio, although some differences between the EM2-SM trend and IC3 in Figs. 1b and 1c exist. Another important feature concerning IC3 is that the data exhibit the extreme enrichment towards the high Sr isotopic ratio only on one side of the major plane (Fig. 1d). Considering these characteristics, a slight but systematic shift of AB along IC3 (point (3) raised above, and seen in Fig. 1f) can be explained by involvement of EM2 or SM-like component (i.e., a continental crustal component), possibly introduced into AB by SM.

A type of MORB-source mantle, which is prevailing in the upper mantle, including the mantle wedge beneath arcs, is fluxed by slab-derived materials such as aqueous fluid, melt, or sometime slab material itself (e.g., Marini *et al.*, 2005), to produce arc magmas. This modification of the source mantle of AB by SM can be evaluated in the compositional space as in Fig. 3. Most of the arcs exhibit individual trends (represented approximately by the arrows in Fig. 3) that can be explained by mixing of a low-IC3 mantle with SM. With increasing IC3, the IC2 value remains broadly constant (Cascade, New Zealand, Scotia) or decreases (Kamchatka, Lesser Antilles), or increases (Mexican), suggesting that the value of IC2 with low-IC3 mantle and slab-derived materials are uncorrelated. For example, in Lesser Antilles, the compositional trend evolves from a near-zero IC2 value to a wider range with increasing IC3, reflecting a large variation in the compositions of subducting sediments including those from the Archean Guiana Highland (White *et al.*, 1985). In Honshu where four plates (Pacific, Philippine Sea, North American and Eurasia) interact, there are two trends reflecting

the complex setting with overlapping subduction and the local heterogeneity of both the mantle and the slab-derived materials (Nakamura and Iwamori, 2009), yet keeping high IC2 values over a wide range of IC3. In any case, the IC2 value at the low-IC3 end of each arc may reflect the inherent sub-arc mantle before being fluxed by slab-derived materials. When the data with high-IC3 values are excluded from Fig. 2, although the number of data decreases, the essential feature with the east-west hemispheres remains unchanged.

Concerning (2), the geographical distribution of IC2 value (Fig. 2) confirms that the east-west discrimination is a visible feature with some details on the geometry of the boundaries between the positive and negative IC2 domains. Based on the geochemical nature, we propose that a fluid mobile component recycled through subduction zones is responsible for IC2: combination of (A) preferential partitioning of Pb into the aqueous fluid derived from a slab through the past subduction and (B) enrichment of U and Th relative to Pb in the residual portion of ancient slab which had experienced dehydration reaction may produce a time-integrated isotopic variation in the direction of IC2 (a positive IC2 directing high $^{204}Pb/^{206}Pb$ value corresponds to (A), whereas a negative IC2 directing low $^{204}Pb/^{206}Pb$ value corresponds to (B)). In this case, a large-scale elevation of the IC2 value in the eastern half of the globe must reflect the past subduction focused in the hemisphere, the most likely beneath a supercontinent.

Between 350 and 200 Ma, the supercontinent Pangea consisted of all the present-day continents distributed over the Northern and Southern Hemispheres (Scotese, 2004), and was surrounded by subduction zones (Fig. 4a). This geometry could have allowed east-west geochemical hemispheres to develop in the mantle, one beneath the supercontinent (pinkish area in Fig. 4) and another beneath the Pantharassic Ocean (bluish area). Focused subduction towards the supercontinent with a subduction velocity 0.1 m/year for ~100 million years can distribute recycled materials beneath the supercontinent of a radius of ~10^7 m. The subducted slabs may stagnate at 660 km or penetrate to the bottom of the mantle sporadically in time and space (Fukao *et al.*, 2001; Grand, 2002), which may hydrate both the upper and lower mantle, partially forming the present-day low-S wave velocity regions near the core-mantle boundary (Iwamori *et al.*, 2010). Then a high-IC2 domain may develop by radiogenic ingrowth over the subsequent ~300 million years to account for the time-evolved isotopic ratios (Iwamori *et al.*, 2010), during which the supercontinent has dispersed towards the present-day configuration. Although the two main subduction zones have migrated apart, expanding the continental area, the planform area of the geochemical domain remains roughly constant without moving with the dispersing continents (Fig. 4b). Accordingly, the geochemical domain has seemingly been anchored to the asthenosphere.

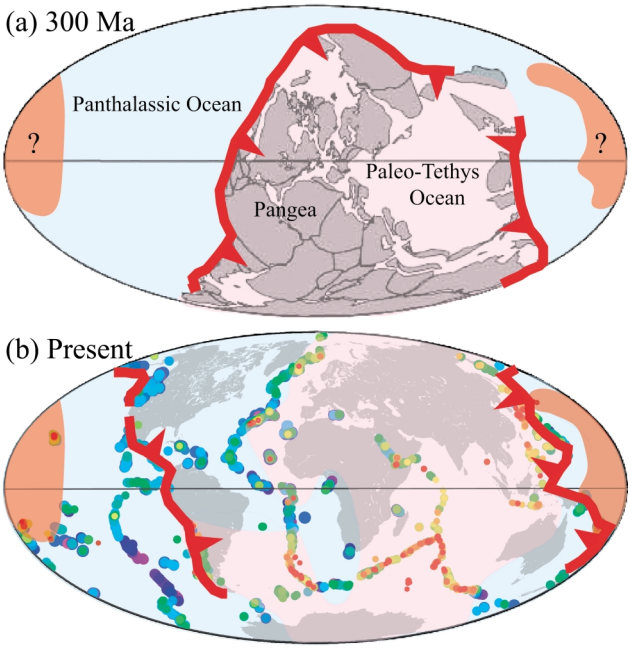

Fig. 4. Evolution of the supercontinent Pangea and the underlying geochemical hemispheres. (a) The possible configuration at 300 Ma, where the pinkish area represents the fluid mobile component-rich mantle developed beneath Pangea, whereas the reddish area represents hypothetical "older domain" developed beneath Rodinia. The bluish area represents the fluid mobile component-poor domain developed beneath the Panthalassic Ocean. (b) The present-day configuration with the observed distribution of IC2 value, based on which the high-IC2 domain (pinkish area with dominantly IC2 > 0) and low-IC2 domain (bluish area with dominantly IC2 < 0) are illustrated.

There are some additional details. Distribution of the negative IC2 domain (i.e., anciently subducted component-poor domain, blue portion in Fig. 4) beneath the western hemisphere, including the American Plates that had been a part of the supercontinent, suggests that dispersion of the continents has occurred asymmetrically more to the west in terms of the geochemical domain. This asymmetricity implies eastward migration of low-IC2 asthenosphere (once beneath the Pantharassic Ocean) relative to the overlying lithosphere or westward lithospheric rotation against the asthenosphere, which is suggested for the preset-day Earth (Ricard *et al.*, 1991). Although the history of rotation is uncertain, if we apply the current rate of 2 cm/year (Ricard *et al.*, 1991) for the last 300 Ma, the resultant westward migration over 6000 km roughly explains that the low-IC2 domain now exists beneath the American Plates (Fig. 4b).

In the southern Pacific, basalts with extreme IC2 val-

ues are observed, known as EM1 (IC2 ~ +5) around Society and HIMU (IC2 ~ –5) around Mangaia (Fig. 1e), based on which the geochemical domain in the Pacific Ocean (Fig. 4b) has been argued to be old (e.g., 0.8 Ga), corresponding to subduction towards the supercontinent Rodinia (Iwamori *et al*., 2010). This possibly old domain seems amalgamating with the new domain (Fig. 4b), indicating that the geochemical domains may change their relative positions by asthenospheric flow. Detailed geometry of the boundaries between the high and low IC2 domains in the Atlantic Ocean also suggests an asthenospheric flow: a low-IC2 domain spreads east down to the Southwest Indian Ridge (Fig. 4b).

In summary, these distributions of the continents and the geochemical domains suggest differential rotation between the lithosphere with continents and the asthenosphere deforming itself, and provide constraints on dynamics and history of the mantle. The Dupal anomaly shares some features with the high IC2 domain in that both involve the Southern Atlantic and Indian Oceans. Concerning the geochemical nature, the role of recycled subducted component has been repeatedly argued for the origin of Dupal anomaly, as a domain contaminated by some type of recycled continental material (see Iwamori *et al*., 2010, and the references therein). However, the Dupal anomaly is defined by three different empirical parameters (ΔSr, Δ7/4 and Δ8/4) that measure compositional distances from a reference line and produce three different contour maps (Hart, 1984), preventing us from defining the Dupal anomaly uniquely. On the other hand, the IC2 domain is based on a statistical criterion that accounts for the five isotopic ratios consistently, and is suitable for global mapping of the multiple component systems. Hart (1984) raised a question based on his pioneering work; "If the anomaly is of ancient parentage where were these continental blocks and oceanic reservoirs in the past? Have they been anchored to the Southern Hemisphere?" With the continuous efforts to accumulate the geochemical data, and by adding the arc basalts to Independent Component Analysis of mantle isotopic variability, we now seem to be able to answer partly this question as above.

Acknowledgments—The authors would like to thank Jun-ichi Kimura and an anonymous reviewer for constructive comments and suggestions, which have been useful to improve clarity of the manuscript, and Hisayoshi Yurimoto for editorial handling.

References

Albarède, F., Telouk, P., Blichert-Toft, J., Boyet, M., Agranier, A. and Nelson, B. (2004) Precise and accurate isotopic measurements using multiple-collector ICP-MS. *Geochim. Cosmochim. Acta* **68**, 2725–2744.

Allègre, C. J., Hamelin, B., Provost, A. and Dupré, B. (1987) Topology in isotopic multispace and origin of the mantle chemical heterogeneities. *Earth Planet. Sci. Lett.* **81**, 319–337.

Beattie, P. (1993) Uranium-thorium disequilibria and partitioning on melting of garnet peridotite. *Nature* **363**, 63–65.

Blichert-Toft, J., Agranier, A., Andres, M., Kingsley, R., Schilling, J.-G. and Albarède, F. (2005) Geochemical segmentation of the Mid-Atlantic Ridge north of Iceland and ridge-hot spot interaction in the North Atlantic. *Geochem. Geophys. Geosys.* **6**, doi:10.1029/2004GC000788.

Brenan, J. M., Shaw, H. F., Ryerson, F. J. and Phinney, D. L. (1995) Mineral-aqueous fluid partitioning of trace elements at 900°C and 2.0 GPa: Constraints on the trace element chemistry of mantle and deep crustal fluids. *Geochim. Cosmochim. Acta* **59**, 3331–3350.

Christensen, U. R. and Hofmann, A. W. (1994) Segregation of subducted oceanic crust in the convecting mantle. *J. Geophys. Res.* **99**, 19867–19884.

Dupré, B. and Allègre, C. J. (1983) Pb–Sr isotope variation in Indian Ocean basalts and mixing phenomena. *Nature* **303**, 142–146.

Flower, M. F. J., Russo, R. M., Tamaki, K. and Hoang, N. (2001) Mantle contamination and the Izu–Bonin–Mariana (IBM) 'high-tide mark': evidence for mantle extrusion caused by Tethyan closure. *Tectonophys.* **333**, 9–34.

Fukao, Y., Widiyantoro, S. and Obayashi, M. (2001) Stagnant slabs in the upper and lower mantle transition region. *Rev. Geophys.* **39**, 291–323.

Grand, S. P. (2002) Mantle shear-wave tomography and the fate of subducted slabs. *Phil. Trans. R. Soc. Lond. A* **360**, 2475–2491.

Green, T. H. (1994) Experimental studies of trace-element partitioning applicable to igneous petrogenesis-Sedona 16 years later. *Chem. Geol.* **117**, 1–36.

Hart, S. R. (1984) A large-scale isotope anomaly in the Southern Hemisphere mantle. *Nature* **309**, 753–757.

Hickey-Vargas, R. (1998) Origin of the Indian Ocean-type isotopic signature in basalts from Philippine Sea Plate spreading centers: An assessment of local versus largescale processes. *J. Geophys. Res.* **103**, 20963–20979.

Hofmann, A. W. (1997) Mantle geochemistry: the message from oceanic volcanism. *Nature* **385**, 219–229.

Hyvärinen, A., Karhunen, J. and Oja, E. (2001) *Independent Component Analysis*. John Wiley & Sons.

Ishizuka, O., Taylor, R. N., Milton, A. and Nesbitt, R. W. (2003) Fluid-mantle interaction in an intra-oceanic arc: constraints from high-precision Pb isotopes. *Earth Planet. Sci. Lett.* **211**, 221–236.

Iwamori, H. and Albarède, F. (2008) Decoupled isotopic record of ridge and subduction zone processes in oceanic basalts by independent component analysis. *Geochem. Geophys. Geosys.* **9**, doi:10.1029/2007GC001753.

Iwamori, H., Albarède, F. and Nakamura, H. (2010) Global structure of mantle isotopic heterogeneity and its implications for mantle differentiation and convection. *Earth Planet. Sci. Lett.* **299**, 339–351.

Keppler, H. (1996) Constraints from partitioning experiments on the composition of subduction-zone fluids. *Nature* **380**, 237–240.

Kessel, R., Schmidt, M. W., Ulmer, P. and Pettke, T. (2005) Trace element signature of subduction-zone fluids, melts and supercritical liquids at 120–180 km depth. *Nature* **437**, 724–727, doi:10.1038/nature03971.

Kogiso, T., Tatsumi, Y. and Nakano, S. (1997) Trace element transport during dehydration processes in the subducted oceanic crust: 1. Experiments and implications for the origin of ocean island basalts. *Earth Planet. Sci. Lett.* **148**, 193–205.

Lehnert, K., Su, Y., Langmuir, C., Sarbas, B. and Nohl, U. (2000) A global geochemical database structure for rocks. *Geochem. Geophys. Geosys.* **1**, doi:10.1029/1999GC000026.

Machida, S., Hirano, N. and Kimura, J.-I. (2009) Evidence for recycled plate material in Pacific upper mantle unrelated to plumes. *Geochim. Cosmochim. Acta* **73**, 3028–3037, doi:10.1016/j.gca.2009.01.026.

Marini, J.-C., Chauvel, C. and Maury, R. C. (2005) Hf isotope compositions of northern Luzon arc lavas suggest involvement of pelagic sediments in their source. *Contr. Mineral. Petrol.* **149**, 216–232, doi:10.1007/s00410-004-0645-4.

McKenzie, D., Stracke, A., Blichert-Toft, J., Albarède, F., Grönvold, K. and O'Nions, R. K. (2004) Source enrichment processes responsible for isotopic anomalies in oceanic island basalts. *Geochim. Cosmochim. Acta* **68**, 2699–2724.

Nakagawa, T., Tackley, P. J., Deschamps, F. and Connolly, J. A. D. (2009) Incorporating self-consistently calculated mineral physics into thermochemical mantle convection simulations in a 3-D spherical shell and its influence on seismic anomalies in Earth's mantle. *Geochem. Geophys. Geosys.* **10**, doi:10.1029/2008GC002280.

Nakamura, H. and Iwamori, H. (2009) Contribution of slab-fluid in arc magmas beneath the Japan arcs. *Gondwana Res.* **16**, 431–445, doi:10.1016/j.gr.2009.05.004.

Nakamura, H., Iwamori, H. and Kimura, J.-I. (2008) Geochemical evidence for enhanced fluid flux due to overlapping subducting plates. *Nature Geosci.* **1**, 380–384, doi:10.1038/ngeo200.

Nebel, O., Münker, C., Nebel-Jacobsen, Y. J., Kleine, T., Mezger, K. and Mortimer, N. (2007) Hf–Nd–Pb isotope evidence from Permian arc rocks for the long-term presence of the Indian-Pacific mantle boundary in the SW Pacific. *Earth Planet. Sci. Lett.* **254**, 377–392, doi:10.1016/j.epsl.2006.11.046.

Pearce, J. A., Stern, R. J., Bloomer, S. H. and Fryer, P. (2005) Geochemical mapping of the Mariana arc-basin system: Implications for the nature and distribution of subduction components. *Geochem. Geophys. Geosys.* **6**, Q07006, doi:10.1029/2004GC000895.

Plank, T. and Langmuir, C. H. (1998) The chemical composition of subducting sediment and its consequences for the crust and mantle. *Chem. Geol.* **145**, 325–394.

Ricard, Y., Doglioni, C. and Sabadini, R. (1991) Differential rotation between lithosphere and Mantle: a consequence of lateral mantle viscosity variations. *J. Geophys. Res.* **96**, 8407–8415.

Rudge, J. F., McKenzie, D. and Haynes, P. H. (2005) A theoretical approach to understanding the isotopic heterogeneity of mid-ocean ridge basalt. *Geochim. Cosmochim. Acta* **69**, 3873–3887.

Salters, V. J. M. and Longhi, J. (1999) Trace element partitioning during the initial stages of melting beneath midocean ridges. *Earth Planet. Sci. Lett.* **166**, 15–30.

Scotese, C. R. (2004) A continental drift flipbook. *J. Geol.* **112**, 729–741.

White, W. M., Dupré, B. and Vidal, P. (1985) Sediment subduction and magma genesis in the Lesser Antilles: isotopic and trace element constraints. *J. Geophys. Res.* **91**, 5927–5941.

Zindler, A., Jagoutz, E. and Goldstein, S. (1982) Nd, Sr and Pb isotopic systematics in a three-component mantle: a new perspective. *Nature* **298**, 519–523.

APPENDIX

Compositions of slab-derived materials ("SM" in Figs. 1 and 3) have been evaluated based on trace element and isotopic compositions of AOC (altered basaltic oceanic crust, Nakamura and Iwamori, 2009) and local sediment columns evaluated for 28 subduction zones (Plank and Langmuir, 1998; White *et al*., 1985). First, trace element compositions of slab-derived aqueous fluids are calculated considering elemental mobility for dehydration of AOC and sediment, respectively (Nakamura *et al*., 2008), and then the AOC-fluid and sediment-fluid are mixed with proportions ranging from zero to unity to obtain the fluid compositions. Similarly, mixing of raw materials (i.e., AOC and sediments) has been evaluated. These mixing curves overlap, and are shown as a broad yellowish zone labeled "SM" in Figs. 1 and 3.